Dissociative photoionization of CH 3 SSCH 3 in the region of 8–25 eV

Su-Yu Chiang, Chien-I Ma, and Der-Jr Shr

Citation: The Journal of Chemical Physics **110**, 9056 (1999); doi: 10.1063/1.478826
View online: http://dx.doi.org/10.1063/1.478826
View Table of Contents: http://scitation.aip.org/content/aip/journal/jcp/110/18?ver=pdfcov
Published by the AIP Publishing

Dissociative photoionization of CH_3SSCH_3 in the region of ~8–25 eV

Su-Yu Chiang,[a] Chien-I Ma, and Der-Jr Shr
Synchrotron Radiation Research Center, No. 1, R&D Road VI, Hsinchu Science-Based Industrial Park, Hsinchu 300, Taiwan, Republic of China

(Received 14 January 1999; accepted 16 February 1999)

The dissociative photoionization of CH_3SSCH_3 has been investigated in the photon energy range of ~8–25 eV with a molecular beam/photoionization mass spectrometry/threshold photoelectron spectrometry system using synchrotron radiation as an ionization source. For dissociation above photon energy of 11.5 eV, six fragment ions of CH_3^+, $C_2H_3^+$, SH_3^+, HCS^+, S_2^+, and $CH_2S_2^+$ were reported for the first time. The photoionization efficiency spectra for the parent ion and for 12 observed fragment ions, CH_3^+, $C_2H_3^+$, SH_3^+, HCS^+, CH_2S^+, CH_2SH^+, CH_3SH^+, $CH_3SH_2^+$, $CH_3SCH_2^+$, S_2^+, $CH_2S_2^+$, and $CH_2S_2H^+$, were measured; their branching ratios as a function of photon energy were derived. Ionization energy of 8.20 ± 0.04 eV for CH_3SSCH_3 and the appearance energy for each fragment ion were determined from the onsets of the photoionization efficiency spectra. Based on the appearance energy and existing thermochemical data, plausible structures of the fragment ions and their neutral counterparts are proposed. Fragmentation mechanisms that involve H migration and structural rearrangement in the dissociative photoionization processes are discussed. © *1999 American Institute of Physics.* [S0021-9606(99)01418-X]

I. INTRODUCTION

Dimethyl disulfide (CH_3SSCH_3) is an important precursor in the atmospheric sulfur chemistry cycles that contribute to formation of acid rain.[1–6] Hence it is of fundamental importance to understand its photochemistry through study of energetics and structures of its photoionization products, and branching ratios as a function of photon energy in various dissociation channels. Numerous experimental measurements and theoretical calculations in the literature establish a reliable thermochemical database of organosulfur molecules, radicals, and ions.[7–25] However, accurate determination of the adiabatic ionization energy (IE) of CH_3SSCH_3 is hindered because of alteration of its geometry upon ionization, and the unimolecular decomposition properties of $CH_3SSCH_3^+$ were studied only in the photon energy range of 8–12 eV.[7–10,26–30]

A value of ~8.3 eV for the IE of CH_3SSCH_3 was determined by photoionization (PI) and photoelectron spectroscopy (PES) in conventional gaseous experiments.[7,27] However, using threshold photoelectron–photoion coincidence (TPEPICO), Butler *et al.*[7] measured the dissociation rates of energy-selected parent ions in channels of formation of $C_2H_5S^+$ and CH_2S^+, and found IE$=7.4\pm0.3$ eV in order to fit the ion dissociation rates with Rice–Ramsperger–Kassel–Marcus (RRKM) theory.[31,32] Li *et al.*[8] detected a small step occurring at 8.18 ± 0.03 eV besides a much stronger step at 8.33 eV in the threshold region of the PI efficiency (PIE) curve of CH_3SSCH_3 seeded in Ar. This new value, 8.18 eV, in fair agreement with a theoretical prediction at 8.15 eV in the same paper,[8] was assigned as the IE of *trans*-$CH_3SSCH_3^+$, whereas the step at 8.33 eV was attributed to formation of *cis*-$CH_3SSCH_3^+$. Later, using low-energy ion–molecule reactions, Leeck and Kenttämaa[10] assigned an IE of 8.0 ± 0.2 eV, close to the 8.18 eV reported by Li *et al.*[8] The adiabatic IE was also corrected from 7.4 ±0.3 to 8.18 ± 0.03 eV following new RRKM calculations.[9] Nevertheless, in a more recent work with a discharge flow coupled to a quadrupole mass spectrometer (QMS) system, no sign of a small step was found near the onset of the PIE curve of CH_3SSCH_3, thus yielding IE$=8.34\pm0.03$ eV again.[30]

Dissociation products of $CH_3SSCH_3^+$ were identified by Butler *et al.*[7] in the photon energy range of 8–12 eV, and the appearance energies (AEs) of six major fragment ions, CH_3SS^+, $C_2H_5S^+$, $CH_3SH_2^+$, CH_3SH^+, CH_3S^+, and CH_2S^+, at 298 K were obtained from the onsets of their respective PIE curves. Through appropriate thermochemical cycles and measured AEs, heats of formation of observed fragment ions were derived; thus their most probable structures were proposed. Among the derived heats of formation, some are substantially smaller than values reported in other experiments. In order to establish independently the heat of formation of CH_2S^+, Ruscic and Berkowitz[20] reexamined the dissociation onsets of $CH_3SSCH_3^+$ on four fragment ions, CH_2S^+, CH_2SH^+, CH_3SH^+, and $CH_3SH_2^+$, but no absolute AEs of these four fragment ions, merely relative shifts between their respective AEs, were determined by matching curvatures of their respective photoion yield curves.

Not long ago, Ma *et al.*[9] reexamined the unimolecular dissociation onset of jet-cooled $CH_3SSCH_3^+$ in the channel forming $CH_3S_2^+$. A clear threshold at 11.07 ± 0.05 eV is significantly greater than 10.15 eV reported by Butler *et al.*,[7] but agrees satisfactorily with Butler's onset at 11.10 eV. Moreover, Ma *et al.* recalculated the RRKM dissociation rates for channels forming $C_2H_5S_2^+$ and $CH_3S_2^+$ using IE$=8.18$ eV and rates of decay of $C_2H_5S_2^+$ measured by Butler *et al.* According to Ma's RRKM result, a kinetic shift at

[a]Corresponding author; electronic mail: schiang@srrc.gov.tw

0.2 eV for the $CH_3S_2^+$ channel was estimated. Based on their onset, kinetic shift, and *ab initio* calculations,[33] they proposed that the most likely isomer of the ion $CH_3S_2^+$ formed at 11.07 eV was CH_2SSH^+, rather than CH_3SS^+ suggested by Butler *et al.*

No data are available on dissociative properties of $CH_3SSCH_3^+$ beyond a photon energy of 12 eV, nor are branching ratios of various dissociation channels reported previously. With this concern and with the discrepancies among heats of formation and structures in the literature for fragment ions of CH_3SS^+ and $C_2H_5S^+$ produced in the photon energy region of 8–12 eV, and among IE values of CH_3SSCH_3, an extensive study of the dissociative photoionization of CH_3SSCH_3 is deemed necessary. In this work, we investigated the dissociative photoionization of CH_3SSCH_3 in the photon energy region of ~8–25 eV using a molecular beam/QMS/TPES setup and synchrotron radiation as an ionization source. The branching ratios of the parent ion and the 12 observed fragment ions as a function of photon energy in the range of ~8–25 eV were measured for the first time. The IE of CH_3SSCH_3 and the AE for each fragment ion were determined from the onsets of the photoionization efficiency spectra. From the determined AEs of these observed fragment ions, new information on the likely structures of the fragment ions and their neutral counterparts is provided. Furthermore, we discuss fragmentation mechanisms involving H migration and structural rearrangement.

II. EXPERIMENT

Dissociative photoionization of CH_3SSCH_3 was performed with a molecular beam/QMS/TPES system, that will be described in detail in a forthcoming publication,[34] using synchrotron radiation as an ionization source. Synchrotron radiation from the 1.5 GeV electron storage ring of the Synchrotron Radiation Research Center (SRRC) in Taiwan is dispersed by a 1 m Seya-Namioka monochromator, which is equipped with three gratings with groove densities of 2400, 1200, and 600 lines/mm to cover a spectral range of 300–3000 Å.[35] Typically, gratings with 600 and 1200 lines/mm and a slit width 0.1–0.2 mm were used in the wavelength region ~500–1550 Å, which provides a wavelength resolution of 1.25–2.5 Å (full width at half maximum) and a photon flux $>10^9$ photons/s. The wavelength of the monochromator was calibrated absolutely on recording photoionization and threshold photoelectron spectra of Ar, and found to be better than 0.2 Å.[36,37] For wavelengths longer than 1050 Å, a LiF window served to eliminate high-order harmonic contamination from the grating. With a grating at 1200 lines/mm, the high-order contribution is about 1%–3% below 1050 Å.

In this experiment, CH_3SSCH_3 vapor carried by He was expanded through a nozzle with a diameter of 0.125 mm and skimmed with two conical skimmers with apertures of 1 and 2 mm to form a cooled sample beam. The total stagnation pressure monitored (MKS baratron) was ~330 Torr (pressure ratio, CH_3SSCH_3:He$\approx$1:10). With a resistive heater, the temperature of the nozzle tip monitored with a Chromel–Alumel thermocouple was kept at 313 ± 1 K to avoid condensation of CH_3SSCH_3. To maintain the vacuum of the beamline, a differential pumping system was installed between the beamline and the ionization chamber; we kept the pressure in the ionization chamber less than 5×10^{-7} Torr when the sample beam was introduced.

The sample in the molecular beam was ionized about 105 mm downstream of the nozzle with the monochromatic synchrotron radiation that intersects the molecular beam at a right angle. The ions and electrons produced were extracted in opposite directions and toward their respective detection axes perpendicular to the plane defined by molecular and photon beams. The ions were mass analyzed with a quadrupole mass spectrometer (Extrel, C50) and detected with an electron multiplier (channeltron) operated in pulse-counting mode. A threshold photoelectron spectrometer with two microchannel plates as detectors served for threshold electron collection. Both ion and electron signals were amplified and counted with a dual-photon counter before being transferred to a computer for further processing. To normalize intensities of the ions and electrons to photon intensity, we placed Ni meshes (90% transmission) at the entrance and exit of the ionization chamber to monitor the variation of the photon flux. The mesh currents were converted to frequencies that were then fed into a second dual-photon counter. All data acquisition processes were controlled with a computer via an IEEE-488 interface.

The mass spectra were measured at wavelengths that correspond to various electronic states of $CH_3SSCH_3^+$. The mass resolution ($m/\Delta m$) was about 150 at $m/z=94$. As no signal at mass greater than that of $CH_3SSCH_3^+$ was detected, all observed fragment ions were considered to originate from dissociative processes of the parent ion. The PIE curves of the parent ion and various fragment ions resulted from measurement of the signal at the respective m/z channels as a function of the wavelength with an increment 4 Å, and were normalized to the photon flux. No attempt was made to accumulate the ion signals of ^{34}S-containing species since these were not abundant. To determine the ionization energy of CH_3SSCH_3 and the appearance energies of all observed fragment ions precisely, we measured the PIE curves near the threshold regions with a wavelength increment of 0.2–1 Å and an accumulation period of 10–45 s/point depending on the abundance of the ions.

The CH_3SSCH_3 sample was obtained from a commercial source (Merck) with a stated purity of 99%; no further purification was made except for freeze–pump–thaw degassing. Noble gases, He and Ar, with purities >99.9995% were used without purification.

III. RESULTS AND DISCUSSION

A. Threshold photoelectron spectrum of CH_3SSCH_3

The TPE spectrum of CH_3SSCH_3 was measured with a wavelength increment of 2 Å in the region of 300–1500 Å (~41–8.3 eV), as shown in Fig. 1. Gratings with groove densities of 2400, 1200, and 600 lines/mm were used in regions of 300–750, 750–1040, and 1050–1500 Å, respectively. The sharp feature at 1080 Å originates from the TPE of He because for this spectrum no LiF filter was installed to

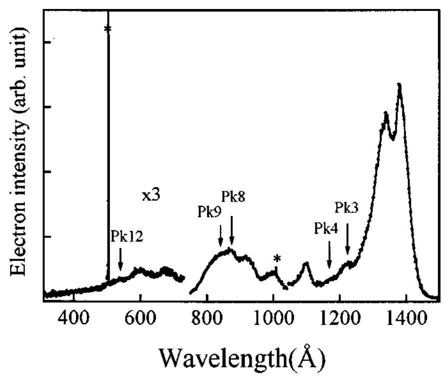

FIG. 1. TPE spectrum of CH_3SSCH_3 in the wavelength region of 300–1500 Å (~41–8.3 eV). This spectrum was measured with a wavelength increment of 2 Å, three gratings with groove densities of 2400, 1200, and 600 lines/mm were used in regions of 300–750, 750–1040, and 1050–1500 Å, respectively. The asterisk (*) marks TPE signals of He originating from excitations of the fundamental and high-order light from the grating, and serves for wavelength calibration.

eliminate high-order light from the grating, but, together with the peak at 504 Å, this feature served for wavelength calibration. Table I lists band maxima in the wavelength and energy in the range of ~8–23 eV. Also noted in Table I are bands of the He I PE spectrum of CH_3SSCH_3 at vertical ionization energies of 8.96, 9.26, 11.26, 12.31, 13.42, 14.35, and 14.75 eV which, according to molecular–orbital calculations, correspond to removal of an electron from $12b$, $13a$, $12a$, $11a$, $11b$, $10b$, and $9b$ molecular orbitals, respectively.[29,36–38]

The TPE spectrum in the region of 650–1550 Å exhibits features similar to those in the PE spectrum, but with different relative intensities, which could be attributed to different Franck–Condon factors.[29,38] In particular, the PE spectrum shows negligible signals in the region of 1120–1240 Å. The signals in the TPE spectrum in this Franck–Condon gap region might be due to autoionization processes that produce low-energy electrons that are detected as threshold photoelectrons.

TABLE I. Band maxima in the threshold photoelectron spectrum of CH_3SSCH_3 in the energy region of ~8–23 eV, compared with literature results of the photoelectron spectrum.

Peak no.	Wavelength (Å)	Energy (eV)	Energy[a] (eV)	Difference (eV)	Character
1	1380.6	8.98±0.02	8.96	0.02	n_S^-
2	1339.6	9.26±0.02	9.26	0.00	n_S^+
3	1226.6	10.11±0.02	⋯	⋯	Autoionization[b]
4	1183.5	10.48±0.03	⋯	⋯	Autoionization[b]
5	1100.4	11.27±0.02	11.26	0.01	σ_{SS}
6	1002.4	12.37±0.03	12.31	0.06	σ_{CS}
7	922.4	13.44±0.03	13.42	0.02	σ_{CS}
8	870.3	14.25±0.04	14.35	−0.1	π_{CH_3}
9	838.3	14.79±0.07	14.75	0.04	π_{CH_3}
10	680.0	18.23±0.09	⋯	⋯	⋯
11	599.4	20.68±0.09	⋯	⋯	⋯
12	540.0	22.96±0.2	⋯	⋯	⋯

[a]Reference 29.
[b]Assigned in this work.

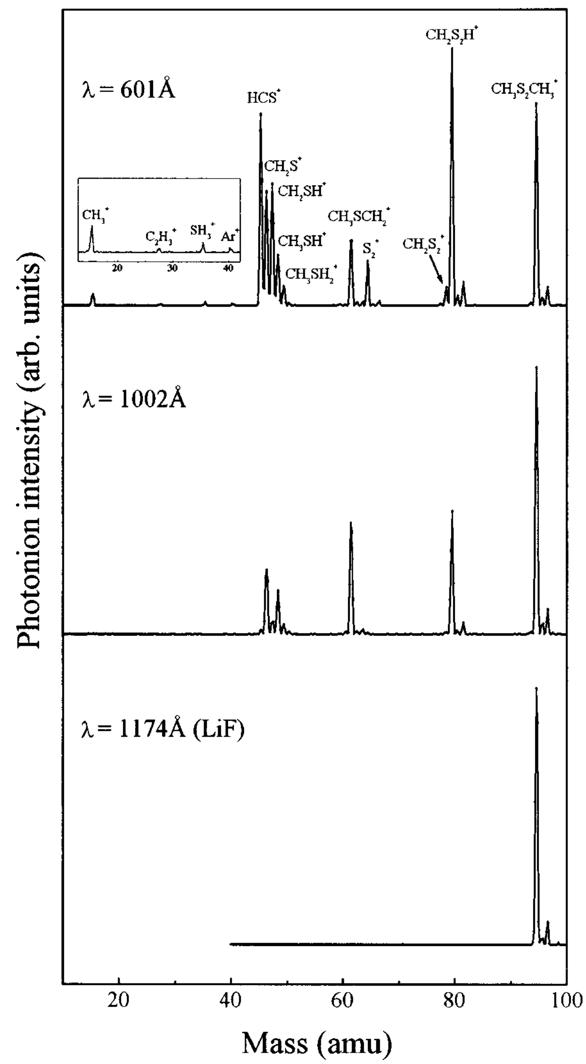

FIG. 2. Fragmentation mass spectra of CH_3SSCH_3 excited at wavelengths of 1174 (10.56 eV), 1002 (12.37 eV), and 601 Å (20.63 eV). At an excitation wavelength of 602 Å, 12 fragment ions of CH_3^+, $C_2H_3^+$, SH_3^+, HCS^+, CH_2S^+, CH_2SH^+, CH_3SH^+, $CH_3SH_2^+$, $CH_3SCH_2^+$, S_2^+, $CH_2S_2^+$, and $CH_2S_2H^+$ were observed. The Ar^+ signal serves for wavelength calibration, and magnified signals of fragment ions of CH_3^+, $C_2H_3^+$, SH_3^+, and Ar^+ are in the inset.

The TPE spectrum in the region of 400–650 Å shows three bands with maxima at 680, 599, and 540 Å, unreported for the previous PE experiments. To ascertain these assignments and to determine vertical energies of these electronic bands, a molecular–orbital calculation is needed. In summary, our TPE spectrum agrees satisfactorily with the previous PE spectrum reported in the literature, except for the newly observed bands at 1226.6, 1183.5, 680.0, 599.4, and 540.0 Å.

B. Primary fragment ions observed

The fragmentation mass spectra of CH_3SSCH_3 excited at wavelengths of 1174 (10.56 eV), 1002 (12.37 eV), and 601 Å (20.63 eV), which correspond to excitation of $CH_3SSCH_3^+$ to various electronic excited states, are shown in Fig. 2. The spectra were scanned with a step of 0.2 amu and a slit width of 100 μm. As can be discerned in Fig. 2, signals due to several new fragment ions appear as the photon energy increases. At an excitation wavelength of 601 Å, 12 fragment ions, separate from sulfur isotopic species, were observed at $m/z = 15$, 27, 35, 45, 46, 47, 48, 49, 61, 64, 78, and 79, corresponding to isomeric structures of CH_3^+, $C_2H_3^+$, SH_3^+, HCS^+, CH_2S^+, CH_3S^+, CH_4S^+, CH_5S^+, $C_2H_5S^+$, S_2^+, $CH_2S_2^+$, and $CH_3S_2^+$, respectively. The fragment ions, CH_3^+, $C_2H_3^+$, SH_3^+, HCS^+, S_2^+, and $CH_2S_2^+$, are reported for the first time. The production of fragment ions at $m/z = 27$ and 61 implies that the parent ion undergoes isomerization before fragmentation. We discuss in Sec. III D isomeric structures of these fragment ions based on our determined AEs and heats of formation of fragment ions and their neutral counterparts reported in the literature.

C. Photoionization efficiency curves and relative branching ratios

Figure 3(a) shows the PIE curves of the parent ion and all observed fragment ions in the wavelength region of 550–1400 Å (22.5–8.9 eV). The PIE curves are normalized with respect to photon flux and scanned linearly in wavelength. The corresponding scale of energy in electron volts is also shown at the top. Since the natural abundance of ^{34}S is substantial, the PIE curves at $m/z = 47$, 48, and 49 were corrected for contributions from ion signals at $m/z = 45$, 46, and 47, respectively. But, no attempt was made to correct the high-order light contribution from the grating, as it is less than 3% and difficult to estimate. Based on the normalized PIE curves, the branching ratios of parent and fragment ions as a function of wavelength are derived and they are depicted in Fig. 3(b), in which the total ion intensity is scaled to 100 for each data point.

To show the correlation between electronic bands and intensity variations of parent and fragment ions, dashed lines indicating vertical transition energies of 11 bands in the TPE spectrum are also depicted in Figs. 3(a) and 3(b). Although the PIE curves fail to exhibit fine feature like those in the TPE spectrum, the variation of intensity among the curves shows phenomena worth noting. In Fig. 3(a), the intensity due to the parent ion increases from threshold to a maximum at ~1180 Å, and then decreases abruptly until ~922 Å, after which it attains a plateau and declines monotonically from ~770 Å toward shorter wavelengths. The stepwise increase of intensity up to 1180 Å follows the onsets of electronic states, and the decrease of intensity from ~1180 Å reflects formation of fragment ions with $m/z = 46$, 47, 48, 49, and 61 from their respective thresholds in the region of 1120–1200 Å, seen in Fig. 3(b). As mentioned before, threshold electron signals were observed in this Franck–Condon gap region; such a phenomenon indicates that autoionization states play an important role in the formation of fragment ions with $m/z = 46$, 47, 48, 49, and 61 at threshold.

Also seen in Fig. 3(a) is that fragment ions with $m/z = 46$, 48, 49, and 61 show similar behavior. Beginning at threshold, the ion signals at $m/z = 46$, 48, 49, and 61 increase and reach a common maximum at ~1090 Å, and then remain nearly constant until ~770 Å, except for the signal at $m/z = 61$ which declines steadily from its maximum toward shorter wavelengths. The nearly constant intensities of fragment ions at $m/z = 46$, 48, and 49 suggest that they are formed through similar dissociation paths, and that their dissociation rates are greater than that of the ion with m/z

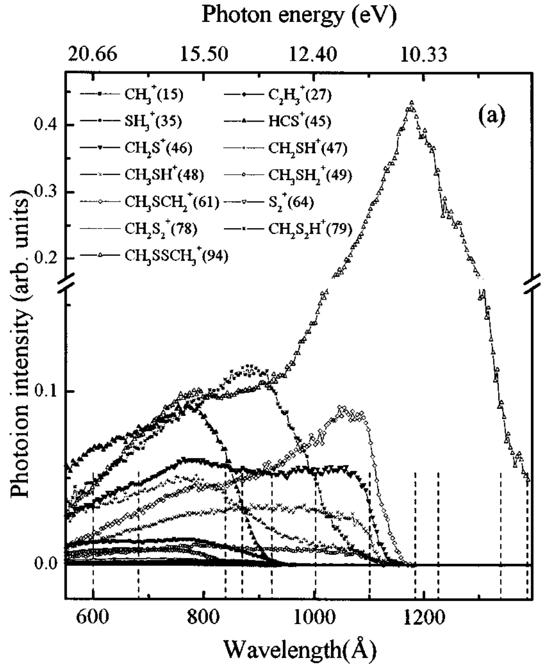

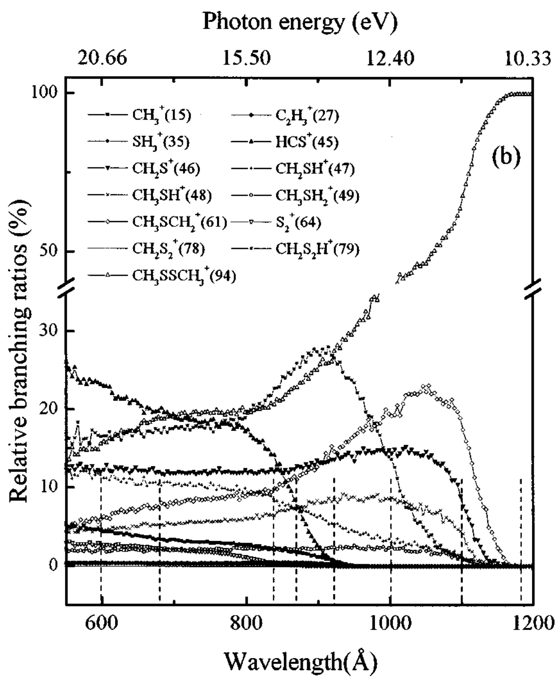

FIG. 3. (a) Normalized PIE curves of $CH_3SSCH_3^+$ and all observed fragment ions in the wavelength region of 550–1400 Å (22.5–8.9 eV). (b) Relative branching ratios of $CH_3SSCH_3^+$ and all observed fragment ions in the wavelength region of 550–1200 Å (22.5–10.3 eV). The m/z ratios of each fragment ion are indicated in parentheses. The total ion intensity is scaled to 100 for the entire wavelength region. Dashed lines, marked at vertical energies of the 11 bands observed in the TPE spectrum, indicate the correlation between these electronic bands and the intensity variation of parent and fragment ions.

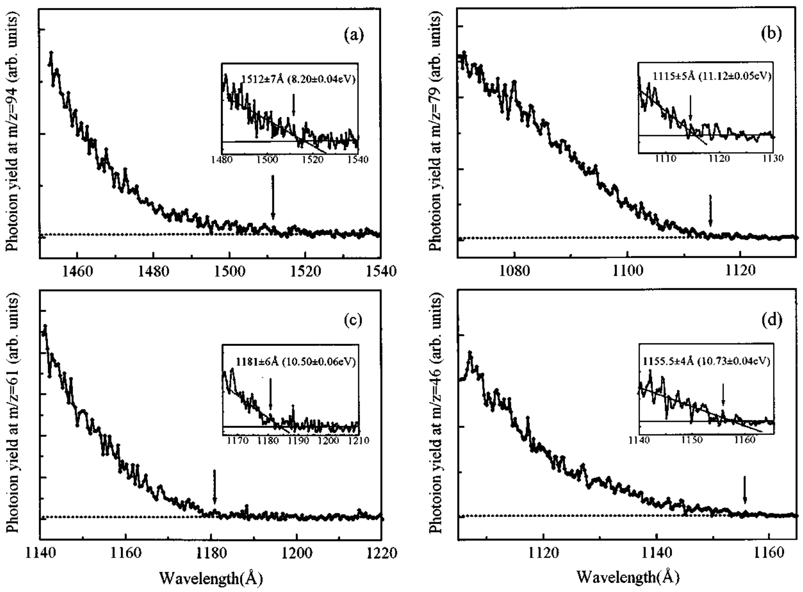

FIG. 4. (a)–(d) Photoion yields of $CH_3SSCH_3^+$ and fragment ions observed at $m/z=79$, 61, and 46, and their respective linearly fitted lines near the threshold region. A LiF window served to eliminate high-order contamination of light from the grating for the fragment ions.

$=61$ as the photon energy increases from their common maximum.

Competition of dissociation channels is observed for pairs of fragments. For example, a decrease of signal for $m/z=61$ is accompanied by an increase of signal for $m/z=79$, and a decrease of signal for $m/z=79$ is accompanied by an increase for an ion with $m/z=45$. This phenomenon could be due to dissociation channels opening as the internal energy of the parent ion increases, or to the onsets of electronic states. However, it is difficult to distinguish these two factors simply from the PIE curves as the photon energy increases because the existence of many excited electronic states complicates identification of formation sources of parent and fragment ions. Measurements of photoelectron–photoion coincidence spectra might reveal a correlation between formation of these fragment ions and ionic electronically excited states.

Fragment ions with $m/z=15$, 27, 35, 45, 64, and 78, as we know, have not been reported previously in dissociation of $CH_3SSCH_3^+$. The proportions of fragment ions produced at $m/z=27$ and 35 are small, less than a 1% contribution, and are thus barely visible in Figs. 3(a) and 3(b). Fragment ions of CH_3^+, HCS^+, S_2^+, and $CH_2S_2^+$ are produced in significant proportions above 800 Å; among them, HCS^+ is the major fragment ion with more than a 20% contribution, seen in Fig. 3(b).

D. Dissociation of $CH_3SSCH_3^+$

1. Ionization and appearance energies

The photoion yields and linearly fitted lines near the threshold region for parent and fragment ions with $m/z=79$, 61, and 46 are shown in Figs. 4(a)–4(d); a LiF window served to eliminate high-order contamination from the grating. The observed onset rises gradually because of a small Franck–Condon factor that reflects an altered conformation upon ionization, the CSSC dihedral angle altering from ~85° to 0° and 180°.[11,26–28] The IE of CH_3SSCH_3 and the AE of each fragment ion were thus determined from signals occurring above the intersection of two linearly fitted lines, one the baseline and the other the onset. AE values estimated in this way represent upper limits due to the possible presence of reverse activation barriers and kinetic shifts, but data treatment of this kind has proved to be useful in general.[39,40]

Table II lists the determined values, proposed dissociation channels, and AEs reported in the literature. As can be seen in Table II, our IE at 1512 ± 7 Å$(8.20\pm0.04$ eV$)$ agrees satisfactorily with values of 8.18 ± 0.03 eV reported by Li *et al.*[8] and 8.0 ± 0.2 eV reported by Leeck and Kenttämaa.[10] The IE at 8.34 ± 0.03 eV determined by discharge flow and a QMS likely reflects their small detection sensitivity.[30] Six dissociation channels, (1), (2), (3), (4), (10), and (11), are observed for the first time, and for other channels, (5), (6), (7), (8), (9), and (12), our AE values significantly exceed literature values.[7] The proposed dissociation products and the reason for the large AE differences are discussed based on our AEs and heats of formation taken from the literature.

2. Proposal of dissociation channels

In general, AEs and heats of formation of a fragment ion and its neutral counterpart are equated as follows:

$$\begin{aligned}\text{AE (fragment ion)} \geqslant & \Delta H_{f0}^0(\text{fragment ion}) \\ & +\Delta H_{f0}^0(\text{neutral partner}) \\ & -\Delta H_{f0}^0(CH_3SSCH_3),\end{aligned} \qquad (1)$$

in which ΔH_{f0}^0 is the heat of formation at 0 K. As the molecular beam cooled CH_3SSCH_3 in the present photoionization experiment, the thermal internal energy of CH_3SSCH_3 was neglected in our calculations. For reference, heats of formation of organosulfur species at 0 K taken from the literature are listed in Table III.[9,14,20,23,41–43] In what follows we discuss properties of these dissociation channels.

a. Dissociation channels of $CH_3SSCH_3^+$ proposed for wavelengths above 1100 Å. For the purpose of discussion, we temporarily assign isomeric structures of $CH_3S_2^+$, $C_2H_5S^+$, CH_5S^+, CH_4S^+, CH_3S^+, and CH_2S^+ to the ob-

TABLE II. Ionization energy of CH_3SSCH_3, appearance energies of fragment ions, proposed structures of some products, and AEs calculated from heats of formation listed in Table III and AEs in the literature.

Dissoc. chn.	Proposed ion	Proposed neutral	Energy[a] (eV)	Energy (eV)[b]	Energy (eV)[c]	Literature[d] (eV)
	$CH_3SSCH_3^+$		8.20 ± 0.04			8.18 ± 0.03[e] 8.33[f]
1	CH_3^+	⋯	12.85 ± 0.05			
2	$C_2H_3^+$	H_2S+SH	13.32 ± 0.05	12.92	(0.40)	
3	SH_3^+	CH_3+CS	12.84 ± 0.05	12.58	(0.26)	
4	HCS^+	⋯	13.24 ± 0.05			
5	CH_2S^+	CH_3SH[g]	10.73 ± 0.04	10.55	(0.18)	10.15 ± 0.08
6	CH_2SH^+	CH_3S	10.82 ± 0.04	10.60	(0.22)	$10.4\ \pm0.1$
7	CH_3SH^+	CH_2S[g]	10.78 ± 0.04	10.61	(0.17)	$10.4\ \pm0.1$
8	$CH_3SH_2^+$	HCS	10.90 ± 0.04	10.68	(0.22)	$10.5\ \pm0.1$
9	$CH_3SCH_2^+$	SH	10.50 ± 0.05	9.94	(0.56)	10.08 ± 0.08
10	S_2^+	$2CH_3$	14.12 ± 0.05	13.85	(0.27)	
11	$CH_2S_2^+$	⋯	12.29 ± 0.10			
12	$CH_2S_2H^+$	CH_3	11.12 ± 0.05	10.85	(0.27)	10.15 ± 0.10 11.07 ± 0.05[h]

[a]Measured in this work.
[b]Calculated from heats of formation listed in Table III.
[c]Difference between the experimental values derived in this work and those calculated.
[d]Reference 7, unless stated otherwise.
[e]Adiabatic IE for $CH_3SSCH_3\rightarrow$*trans*-$CH_3SSCH_3^+$, Ref. 8.
[f]Adiabatic IE for $CH_3SSCH_3\rightarrow$*cis*-$CH_3SSCH_3^+$, Ref. 8.
[g]Violation of Stevenson's rule.
[h]Reference 9.

served fragment ions at $m/z=79$, 61, 49, 48, 47, and 46, respectively, since several isomeric structures exist for each observed fragment ion of a particular m/z ratio.

(1) CH_5S^+, CH_4S^+, CH_3S^+, and CH_2S^+ ($m/z=49-46$): Four fragment ions, CH_5S^+, CH_4S^+, CH_3S^+, and CH_2S^+, with $m/z=49-46$, are observed with their respective AEs, 10.90 ± 0.04, 10.78 ± 0.04, 10.82 ± 0.04, and 10.73 ± 0.04 eV. These values are significantly higher than those of Butler *et al.*, 10.5 ± 0.1, 10.4 ± 0.1, 10.4 ± 0.1, and 10.15 ± 0.08 eV,[7] and the cause of this large discrepancy, more than 0.3 eV, is unclear.

TABLE III. Auxiliary heats of formation of selected organosulfur species from the specified sources.

Molecule	ΔH_{f0}^0 (kcal/mol)[a]
CH_3SSCH_3	-1.6
CH_3^+	262
CH_3	35.6
CS	63
HCS	71.7[b]
HCS^+	243.9[b]
CH_2S	28.3[b]
CH_2S^+	244.5[b]
CH_2SH^+	211.5[b]
CH_3S	31.44[c]
CH_3SH	-2.9
CH_3SH^+	214.8
$CH_3SH_2^+$	173
CH_3S_2	17.8[d]
$CH_2S_2H^+$	213[e]
$C_2H_3^+$	267.9
$CH_3SCH_2^+$	195.1[f]
SH	32.6
H_2S	-4.2
SH_3^+	190
S_2^+	246.4
CH_4	-16.0

[a]Reference 42, unless stated otherwise.
[b]Reference 20.
[c]References 14 and 43.
[d]Reference 41.
[e]Reference 9.
[f]Reference 23

Despite differences in the absolute AE, the differences in our AE for adjacent masses, $\Delta E(48,49)=0.12$, $\Delta E(47,48)=-0.04$, and $\Delta E(46,47)=0.09$ eV, are close to the latter two quantities determined by Butler *et al.*, 0.0 and 0.1 eV.[7] Our values are also in agreement with values of 0.108 ± 0.035, 0.000 ± 0.030, and 0.068 ± 0.030 eV obtained by Ruscic and Berkowitz with a curve-matching method.[20]

Upper limits of heats of formation of these four fragment ions are derived using Eq. (1) based on our AEs and well known heats of formation of the most stable structures of proposed neutral counterparts of HCS, CH_2S, CH_3S, and CH_3SH listed in Table III.[14,20,42–43] The ΔH_{f0}^0 of these four fragment ions calculated in this work are 178.1, 218.7, 216.5, and 248.7 kcal/mol, near the reported values of 173, 214.8, 211.5, and 244.5 kcal/mol, corresponding to $CH_3SH_2^+$, CH_3SH^+, CH_2SH^+, and CH_2S^+, respectively.[20,42] The differences between our calculated value ΔH_{f0}^0 and the literature value for each fragment ion are almost constant at 5.1, 3.9, 5.0, and 4.2 kcal/mol, and with the average being 4.6 ± 0.7 kcal/mol (0.2 ± 0.03 eV). Our values, consistently higher than literature values, are rationalized by the presence of kinetic shifts and reverse activation energies for formation of these fragment ions, as mentioned earlier. Thus, we propose $CH_3SH_2^+$, CH_3SH^+, CH_2SH^+, and CH_2S^+ as the most likely structures of fragment ions observed at $m/z=49$, 48, 47, and 46, respectively.

As CH_3SH^+ and CH_2S are the only plausible structures on the basis of energy considerations and the available thermochemical data in the literature, the fragmentation channels of $CH_3SH^+ + CH_2S$ and $CH_2S^+ + CH_3SH$ proposed here do not follow Stevenson's rule. Our assignments for these channels are consistent with those of Ruseic and Berkowitz that were determined from the relative shifts between the respective AEs of fragmentation channels.[20] Butler's assignment for CH_2SH^+ is also consistent with ours, but not for $CHSH^+$ and $CH_2SH_2^+$.[7] A possible explanation is that their values at 170.0, 216.2, 208.0, and 234.1 kcal/mol derived from their low AEs are lower than the literature values, except for 216.2 kcal/mol, which is probably due to an adopted value that is too low, $\Delta H_{f0}^0(CH_2S) = 25.1$ kcal/mol, for the neutral.

(2) $C_2H_5S^+$ ($m/z = 61$): The AE of $C_2H_5S^+$ at 10.50 ± 0.05 eV determined in this work is 0.42 eV higher than the 10.08 eV reported at 298 K, but near the value of 10.28 eV at 0 K derived from statistical fitting of decay rates by Butler *et al.*[7] Regarding the RRKM dissociation rates calculated by Ma *et al.*,[9] a large kinetic shift for the channel forming $C_2H_5S^+$ is expected due to the very tight transition structure which leads to an energy dependence of the dissociation rate rising very slowly with excess energy. A kinetic shift of 0.28 eV is derived if we take the difference between our AE at 10.50 eV and the IE at 8.20 eV of CH_3SSCH_3 and subtract from it the activation energy at 2.02 eV obtained from the RRKM calculation by Ma *et al.*[9] This value agrees satisfactorily with the 0.28 eV derived from the RRKM/QET (quasi-equilibrium theory) decay rates calculated by Butler *et al.*[7] Using our new AE at 10.50 eV, the derived kinetic shift of 0.28 eV, and heats of formation of SH and CH_3SSCH_3 at 0 K listed in Table III, we obtain $\Delta H_{f0}^0(C_2H_5S^+) \leq 201$ kcal/mol from Eq. (1). Compared with theoretical predictions $\Delta H_{f0}^0 = 236.5$ ($CH_3CH_2S^+$), 192.6 (*cis*-CH_3CHSH^+), 192.6 (*trans*-CH_3CHSH^+), and 195.3 ($CH_3SCH_2^+$) kcal/mol, our value is nearer 195.3 ($CH_3SCH_2^+$) kcal/mol.[23] Thus, we assign the isomer $CH_3SCH_2^+$ as the most probable structure, consistent with results from collisional activation, PD–PI, and theoretical prediction.[7,44,45]

(3) $CH_3S_2^+$ ($m/z = 79$): The AE of $CH_3S_2^+$ at 11.12 ± 0.05 eV determined here is significantly higher than the weak onset at 10.15 eV reported by Butler *et al.*,[7] but agrees with their strong onset at 11.10 eV. Our value also agrees with 11.07 eV reported for photoionization of jet-cooled CH_3SSCH_3 by Ma *et al.*[9] Ma *et al.* estimated a large kinetic shift of 0.2 eV for the channel forming $CH_3S_2^+$, and thus derived $\Delta H_{f0}^0(\text{fragment ion}) = 213$ kcal/mol, near $\Delta H_{f0}^0(CH_2SSH^+) = 211$ kcal/mol predicted from their *ab initio* calculation. With this result, they claim the structure of CH_2SSH^+ instead of CH_3SS^+ proposed by Butler *et al.* to be the most likely structure formed near the onset at 11.07 eV. As the kinetic shift cannot be estimated from our measured AE alone, the structure of CH_2SSH^+ proposed by Ma *et al.* was adopted in Table II.

Formation of CH_2SSH^+ implies that the dissociation channel proceeds through a transition structure involving H migration. We note that the proposed fragment ions of $CH_3SH_2^+$, CH_3SH^+, and CH_2SH^+, from a comparison with ΔH_{f0}^0 in the literature, seem to involve H transfers for their formation, too. The average value of the ΔH_{f0}^0 difference between our values and the literature values for $CH_3SH_2^+$, CH_3SH^+, and CH_2SH^+ is 0.2 eV, close to the kinetic shift for the channel to form CH_2SSH^+ according to the RRKM calculation. A perfect match of both values and the common phenomenon involving H transfers mutually support assignments to CH_2SSH^+, $CH_3SH_2^+$, CH_3SH^+, and CH_2SH^+.

b. Dissociation channels of $CH_3SSCH_3^+$ proposed for wavelengths below 1100 Å. Six fragment ions with $m/z = 15$, 27, 35, 45, 64, and 78 were observed and assigned as CH_3^+, $C_2H_3^+$, SH_3^+, HCS^+, S_2^+, and $CH_2S_2^+$, respectively. These fragment ions are formed at dissociation energies much higher than those for the dissociation channels discussed above. With more dissociation channels in competition, the kinetic shifts for channels producing these fragment ions are expected to be large and more difficult to evaluate. Moreover, as these fragment ions are observed for the first time, no relevant datum such as *ab initio* molecular orbital calculations and dissociation rates is available to aid in the explanation of dissociation properties. It becomes difficult to assign neutral partners solely from the determined AE, let alone derivation of heats of formation of these fragment ions. Therefore, we simply list these fragment ions and some neutral fragments in Table II, and discuss them briefly in what follows.

To form S_2^+, loss of two CH_3 groups is the most direct and simple way. If this is the case, these two CH_3 losses must be consecutive, which means that at least part of the $m/z = 79$ ion must be the unrearranged $CH_3S_2^+$ ion formed at photon energies higher than the 11.12 eV onset. On the basis of an energy consideration, two three-body formation processes, $SH_3^+ + CH_3 + CS$ and $C_2H_3^+ + H_2S + SH$, are also assumed. Formation of $C_2H_3^+$ likely occurs through a tight transition structure to form a C–C bond, while SH_3^+ may involve H transfer.

IV. CONCLUSIONS

Dissociative photoionization of CH_3SSCH_3 into channels to form CH_3^+, $C_2H_3^+$, $CH_3SCH_2^+$, HCS^+, SH_3^+, CH_2S^+, CH_2SH^+, CH_3SH^+, $CH_3SH_2^+$, S_2^+, $CH_2S_2^+$, and $CH_2S_2H^+$ is effected with a molecular beam/QMS/TPES setup coupled to a synchrotron light source. According to measured photoionization efficiency spectra of the parent ion and 12 fragment ions, the branching ratios of these ions as a function of photon energy were derived in the photon energy region at ~8–25 eV. The IE of CH_3SSCH_3 and the AEs of observed fragment ions were determined from signals occurring above the intersection of the baseline and the rising edge, both fitted to a line by least squares. The AEs thus derived for formation of CH_2S^+, CH_2SH^+, CH_3SH^+, $CH_3SH_2^+$, and $CH_2S_2H^+$ are more consistent with recent studies of CH_3SSCH_3 and similar molecules. Based on the determined AE and existing thermochemical data, plausible structures of some fragment ions and their neutral counterparts were proposed. Isomerization instead of simple cleavage of the C–S bond or the S–S bond seems to be a common step in these dissociative processes.

ACKNOWLEDGMENTS

One of the authors (S.-Y.) is grateful to Professor T. Baer for reading their manuscript and for helpful comments. This work was supported by Synchrotron Radiation Research Center and National Science Council of the Republic of China under Contract No. NSC87-2613-M-213-019.

[1] R. P. Wayne, *Chemistry of Atmospheres* (Clarendon, Oxford, 1991).
[2] M. O. Andreae and H. Raemdonck, Science **221**, 744 (1983).
[3] F. Yin, D. Grosjean, and J. H. Seinfeld, J. Geophys. Res. **91**, 14417 (1986).
[4] J. G. Calvert and J. N. Pitts, *Photochemistry* (Wiley, New York 1996).
[5] S. D. Thompson, D. G. Carrol, F. Watson, M. O'Donnell, and S. P. McGlynn, J. Chem. Phys. **45**, 1367 (1966).
[6] P. M. Rao and A. R. Knight, Can. J. Chem. **46**, 2462 (1968).
[7] J. J. Butler, T. Baer, and S. A. Evans, J. Am. Chem. Soc. **105**, 3451 (1983).
[8] W.-K. Li, Z.-X. Ma, C.-L. Liao, and C. Y. Ng, J. Chem. Phys. **99**, 8440 (1993).
[9] Z.-X. Ma, C.-L. Liao, C. Y. Ng, Y.-S. Cheung, W.-K. Li, and T. Baer, J. Chem. Phys. **100**, 4870 (1994).
[10] D. T. Leeck and H. I. Kenttämaa, Org. Mass Spectrom. **29**, 106 (1994).
[11] J. J. Butler and T. Baer, J. Am. Chem. Soc. **104**, 5016 (1982).
[12] J. M. Nicovich, K. D. Kreutter, C. A. van Dijk, and P. H. Wine, J. Phys. Chem. **96**, 2518 (1992).
[13] J. J. Butler and T. Baer, Org. Mass Spectrom. **18**, 248 (1983).
[14] B. Ruscic and J. Berkowitz, J. Chem. Phys. **97**, 1818 (1992).
[15] S. Nourbakhsh, K. Norwood, H.-M. Yin, C.-L. Liao, and C. Y. Ng, J. Chem. Phys. **95**, 946 (1991).
[16] S. Nourbakhsh, K. Norwood, G.-Z. He, and C. Y. Ng, J. Am. Chem. Soc. **113**, 6311 (1991).
[17] R. H. Nobes and L. Radom, Chem. Phys. Lett. **189**, 554 (1992).
[18] S. Nourbakhsh, H.-M. Yin, C.-L. Liao, and C. Y. Ng, Chem. Phys. Lett. **183**, 348 (1991).
[19] C.-W. Hsu and C. Y. Ng, J. Chem. Phys. **101**, 5596 (1994).
[20] B. Ruscic and J. Berkowitz, J. Chem. Phys. **98**, 2568 (1993).
[21] S. Nourbakhsh, C.-L. Liao, and C. Y. Ng, J. Chem. Phys. **92**, 6587 (1990).
[22] H. Q. Zhao, Y.-S. Cheung, C.-L. Liao, and C. Y. Ng, J. Chem. Phys. **104**, 130 (1996).
[23] Z.-X. Ma, C.-L. Liao, H.-M. Yin, C. Y. Ng, S.-W. Chiu, N. L. Ma, and W.-K. Li, Chem. Phys. Lett. **213**, 250 (1993).
[24] J. E. Stevens, K. F. Freed, and M. F. Arendt, J. Chem. Phys. **101**, 4832 (1994).
[25] S. Nourbakhsh, K. Norwood, H.-M. Yin, C.-L. Liao, and C. Y. Ng, J. Chem. Phys. **95**, 5014 (1991).
[26] R. J. Colton and J. W. Rabalais, J. Electron Spectrosc. Relat. Phenom. **3**, 345 (1974).
[27] A. D. Baker, M. Brisk, and M. Gellender, J. Electron Spectrosc. Relat. Phenom. **3**, 227 (1974).
[28] K. Kimura and K. Osafune, Bull. Chem. Soc. Jpn. **48**, 2421 (1975).
[29] K. Kimura, S. Katsumata, Y. Achiba, Y. Yamazaki, and S. Iwata, *Handbook of He I Photoelectron Spectra of Fundamental Organic Molecules* (Japan Scientific Society, Tokyo, 1980).
[30] W.-C. Hung, M.-Y. Shen, Y.-P. Lee, N.-S. Wang, and B.-M. Cheng, J. Chem. Phys. **105**, 7402 (1996).
[31] T. Baer and W. L. Hase, *Unimolecular Reaction Dynamics: Theory and Experiments* (Oxford University Press, New York, 1996).
[32] P. J. R and K. A. Holbrook, *Unimolecular Reactions* (Wiley, London, 1972).
[33] Y.-S. Cheung, W.-K. Li, and C. Y. Ng, J. Mol. Struct. **339**, 25 (1995).
[34] S. Y. Chiang and C.-I Ma (unpublished).
[35] P.-C. Tseng, T.-F. Hsieh, Y.-F. Song, K.-D. Lee, S.-C. Chung, C.-I. Chen, H.-F. Lin, T.-E. Dann, L.-R. Huang, C.-C. Chen, J.-M. Chuang, K.-L. Tsang, and C.-N. Chang, Rev. Sci. Instrum. **66**, 1815 (1995).
[36] K. Yoshino, J. Opt. Soc. Am. A **60**, 1220 (1970).
[37] R. E. Huffman, Y. Tanaka, and J. C. Larrabee, J. Chem. Phys. **39**, 902 (1963).
[38] A. Yokozeki and S. H. Bauer, J. Phys. Chem. **80**, 618 (1976).
[39] B. P. Tsai, T. Baer, A. S. Werner, and S. F. Lin, J. Phys. Chem. **79**, 570 (1975).
[40] H. Shiromaru, Y. Achiba, K. Kimura, and Y. T. Lee, J. Phys. Chem. **91**, 17 (1987).
[41] Z.-X. Ma, C.-L. Liao, C. Y. Ng, N. L. Ma, and W.-K. Li, J. Chem. Phys. **99**, 6470 (1993).
[42] G. Lias, J. E. Bartmess, J. L. Holmes, R. D. Levin, and W. G. Mallard, J. Phys. Chem. Ref. Data **17**, Suppl. No. 1 (1988).
[43] J. M. Nicovich, K. D. Kreutter, C. A. van Dijk, and P. H. Wine, J. Phys. Chem. **96**, 2518 (1992).
[44] W. J. Borer, W. D. Weringa, and W. C. Nieuwpoort, Org. Mass Spectrom. **14**, 543 (1979).
[45] B. van der Graaf and F. W. Mc Lafferty, J. Am. Chem. Soc. **99**, 6806 (1977).